A SONIC METHOD FOR PETROGRAPHIC ANALYSIS

Thesis for the Degree of M. S.
MICHIGAN STATE UNIVERSITY
STEPHEN EDWARD TILMANN
1974

A SONIC METHOD FOR PETROGRAPHIC ANALYSIS

by

Stephen Edward Tilmann

A THESIS

Submitted to
Michigan State University
in partial fulfillment of the requirements
for the degree of

MASTER OF SCIENCE

Department of Geology

1974

ACKNOWLEDGMENTS

To Dr. Hugh Bennett, my thesis advisor, for his patience and guidance; to Dr. Tom Vogel, for first arousing my curiosity in this subject, and his time spent with me in the field; to Dr. Bob Ehrlich, for giving me a perspective; to Adrian Bass, for moral encouragment; and to those friends of mine in the Department, for making this experience, I gratefully extend my acknowledgments.

A Sonic Method for Petrographic Analysis

STEPHEN E. TILMANN AND HUGH F. BENNETT

Department of Geology, Michigan State University, East Lansing, Michigan 48824

A sonic method as a tool for detecting and describing preferred crystallographic orientation has been proposed by Bennett (1972). The Q ellipsoid is a theoretical surface whose magnitude for any direction is the sum of the squares of the three seismic wave phase velocities for that direction. The orientation of the ellipsoid relative to the sample is controlled by crystal orientation and structural effects of the sample. For completely isotropic samples the Q surface is a sphere; for anisotropic samples the Q surface is ellipsoidal. Sample homogeneity is testable by the closeness of fit of the velocity data to the ellipsoidal surface. In this respect, crystal aggregates can be considered to behave as elastic long-wave equivalents to single crystals. The baraboo quartzite, a Grenville marble, and a plastically deformed granite boulder are analyzed according to the Q ellipsoid technique. Optical analysis is performed on the quartzite and marble. The oriented optical indicatrixes for the individually measured crystals are summed, an ellipsoidal surface characterizing the preferred crystal orientation direction of the sample thus being produced. For the quartzite, which is nearly isotropic, the optical surface and the sonic surface closely coincide. This situation is evidence that the sonic orientation accurately reflects the subtle crystallographic orientation. The marble displays a strong crystallographic orientation, as well as a pronounced micaceous layering. The orientation of the Q ellipsoid reflects the net effect of this structural fabric and the crystallographic fabric. The granitic boulder was plastically deformed into an ellipsoidal shape. The shape axes and the Q ellipsoid axes closely coincide, the indication being that the Q ellipsoid technique may be useful in describing regional tectonic forces.

The concept of the Q ellipsoid as a tool for detecting and describing preferred crystallographic orientations has been developed by *Bennett* [1972]. The purpose of this paper is to test this seismic model with empirical data gathered from several rock types.

The Q ellipsoid is a theoretical surface whose value for any particular direction is the sum of the squares of the three seismic wave type phase velocities in that direction. It has been proved that the principal axes of the Q ellipsoid always coincide with the optical indicatrix axes for a single crystal in the cubic through orthorhombic systems [*Bennett*, 1972]. For cubic crystals the Q surface reduces to a sphere. For uniaxial crystals the Q surface is an ellipsoid of revolution, and for biaxial crystals the Q surface is a triaxial ellipsoid.

If a crystal aggregate is considered as an elastic long-wave equivalent to a single crystal, then the locus of values, of which each value is the sum of the squares of the three seismic wave velocities for any particular direction, should be represented by an ellipsoidal surface; i.e., the material behaves as a homogeneous pseudosingle crystal. Further, the principal axes of this ellipsoid would be controlled by preferred crystallographic orientation and structural effects within the rock material [*Bennett*, 1972]. Thus, if the Q surface is ellipsoidal, then (1) the material is homogeneous and anisotropic, (2) the principal anisotropic directions are described by the ellipsoid principal axes, and (3) the percent difference between the ellipsoid principal axes is a measure of the degree of elastic anisotropy, which is controlled by anisotropic crystal orientation and structural effects.

The concept of the Q ellipsoid need not be restricted to rock materials of a single phase. Indeed an advantage of the Q ellipsoid concept is that a multiphase material can be treated as a pseudosingle crystal in terms of elastic behavior and crystallographic orientation.

It should be pointed out that the P wave velocity surface (also the S_1 and S_2 surfaces) need not conform to any simple geometric shape. For rock materials the three velocity surfaces could be controlled primarily by structural effects, such as microfractures, and ap-

pear to be unrelated to any preferred crystal orientation within the material. This condition may be more noticeable where orientations are weak and contribute less to the anisotropy. Also, since the P wave or S wave velocity surfaces may be quite complex in shape, the maximum value chosen from just a few measurements may not be the true velocity surface maximum.

MODEL

The calculated value Q_i' of the Q ellipsoid for the ith direction is given by

$$Q_i = Q_i'/\rho = (V_1^2 + V_2^2 + V_3^2)_i \qquad (1)$$

where ρ is the material density, V_1 is the P wave velocity in the ith direction, and V_2 and V_3 are the velocities of the two orthogonally polarized shear waves for the ith direction [*Bennett*, 1972]. By defining a polarization plane as the plane that contains the propagation direction and shear wave particle motion, it can be stated that the two polarization planes are nearly orthogonal for any propagation direction. Thus the values of V_2 and V_3 can usually be measured unambiguously for any particular direction [*Tilmann and Bennett*, 1973]. Since the density term is constant, it may be incorporated into the Q_i' term without affecting the shape or the orientation of the Q ellipsoid. Thus the calculated value of the Q ellipsoid in the ith direction will be referred to as Q_i.

The least squares value Q_{LS_i} of the Q ellipsoid for the ith direction is given by

$$Q_{LS_i} = l_i^2\alpha_{11} + m_i^2\alpha_{22} + n_i^2\alpha_{33} + 2m_in_i\alpha_{23} + 2n_il_i\alpha_{31} + 2l_im_i\alpha_{12} \qquad (2)$$

where (l_i, m_i, n_i) are the directional cosines of the ith direction relative to any orthogonal set of axes x, y, and z. In practice the x, y, and z axes are conveniently chosen relative to the sample being analyzed. The α terms are the elements of a 3×3 symmetric ellipsoid matrix.

The elements of the α matrix are determined by the least squares method outlined by *Nye* [1957]. This procedure is based on the matrix equation relating the Q_i values to the directional cosine matrix θ and the α matrix by

$$\mathbf{Q} = \boldsymbol{\theta}\boldsymbol{\alpha} \qquad (3)$$

The Q matrix elements are the measured Q_i values from (1). The θ matrix is constructed by using the l, m, and n coefficients of (2). The α matrix is then determined by solving (3) for α, resulting in

$$\boldsymbol{\alpha} = (\boldsymbol{\theta}_t\boldsymbol{\theta})^{-1}\boldsymbol{\theta}_t\mathbf{Q} \qquad (4)$$

This is the computational form for determining the α matrix. (See *Nye* [1957, pp. 164–165] for a more complete treatment of this procedure.)

The principal axes of the Q ellipsoid are found by the successive approximation method [*Nye*, 1957]. The procedure entails successive relocation of a vector normal to the surface of the ellipsoid until it corresponds to the minor axis. By inverting the α matrix the major axis is similarly located. The intermediate axis is the cross product of the major and minor axes. By using these directional cosines of the major, minor, and then intermediate axes in (2), the magnitude of these axes is easily determined. (Also see *Nye* [1957, pp. 165–168] for a more complete treatment of this procedure.)

Comparison of the measured ellipsoidal values Q_i and the calculated ellipsoidal values Q_{LS_i} provides a test for sample homogeneity. The values of interest are, first,

$$\sigma_{\bar{m}} = \left[\sum_{i=1}^{n} (Q_i - Q_{\bar{m}})^2/n\right]^{1/2} \qquad (5)$$

where Q_i is the measured ellipsoidal value in the ith direction (1), $Q_{\bar{m}}$ is the arithmetic mean measured value, and n is the number of propagation directions i measured; second,

$$\sigma_{\bar{m}_c} = \left[\sum_{i=1}^{n} (Q_{LS_i} - Q_{\bar{m}})^2/n\right]^{1/2} \qquad (6)$$

where Q_{LS_i} is the calculated ellipsoidal value (2) in the ith direction; and, third,

$$\sigma_e = \left[\sum_{i=1}^{n} (Q_i - Q_{LS_i})^2/n\right]^{1/2} \qquad (7)$$

The standard deviation $\sigma_{\bar{m}}$ can be thought of as the deviation of the measured ellipsoidal values from the best-fit sphere to the measured values, $\sigma_{\bar{m}_c}$ is the deviation of the calculated ellipsoidal values from the best-fit sphere, and σ_e is the deviation between the measured and the calculated ellipsoidal values. If all the data

points fall exactly on the ellipsoidal surface, then $\sigma_e = 0$, and $\sigma_{\bar{m}e} = \sigma_{\bar{m}}$.

Sample homogeneity and elastic behavior as a pseudosingle crystal are indicated by the relationship

$$\sigma_{\bar{m}} \geq \sigma_{\bar{m}e} > \sigma_e \tag{8}$$

Sample inhomogeneity is indicated by the relationship

$$\sigma_{\bar{m}} > \sigma_e > \sigma_{\bar{m}e} \tag{9}$$

The inhomogeneity may be in the form of variance of the preferred crystal orientation within the sample or irregular compositional or structural differences within the sample. Inhomogeneity is not consistent with the concept of elastic behavior as a pseudosingle crystal.

TEST

The baraboo quartzite, a Grenville marble, and a plastically deformed granitic boulder were analyzed according to the Q ellipsoid technique. The measuring apparatus used for determining the elastic velocities is described by *Tilmann and Bennett* [1973]. In addition, optical petrofabric analyses were performed on the quartzite and marble.

The quartzite is an essentially pure quartz rock that has undergone slight metamorphism. In hand sample and thin section, no obvious structure was observed that would influence the elastic anisotropy. The marble comprises calcite and a well-defined micaceous layering. The granite boulder has been plastically deformed during metamorphism. The shape of the boulder is roughly that of a triaxial ellipsoid, with the minor axis normal to the plane of outcrop foliation.

TABLE 1. Optical Ellipsoid Axes

Magnitude	Directional Cosines	Symbol
	Quartzite	
41.98	(-0.986, 0.155, 0.058)	M_0
41.82	(0.161, 0.983, 0.087)	m_0
41.94	(0.043, -0.095, 0.995)	I_0
	Marble	
12.46	(0.398, -0.859, 0.322)	M_0
12.10	(0.150, 0.285, 0.947)	m_0
12.20	(0.965, 0.425, 0.015)	I_0

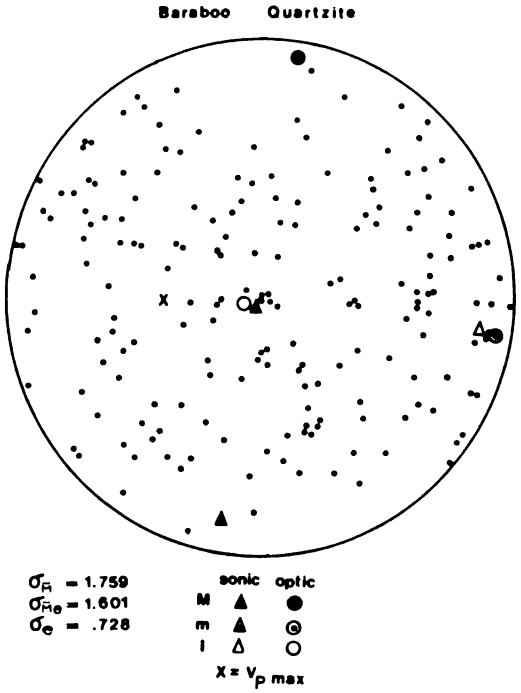

Fig. 1. Equal-area projection of 200 quartz c axes for the baraboo quartzite. The direction of the observed maximum P wave velocity, the optical surface, and the sonic Q ellipsoid principal axes are also plotted, M, m, and I being the ellipsoidal major, minor, and intermediate principal axes, respectively. Close coincidence between the axes of the two surfaces indicates that the orientation of the Q ellipsoid describes the preferred crystallographic orientation.

Baraboo quartzite. The results of the optical petrofabric analysis on the quartzite are presented in Figure 1. This diagram is an equal-area projection of the measured quartz c axes. This projection was not contoured in order to emphasize the diffuse nature of the orientation. The oriented optical indicatrixes of the individually measured crystals were summed in order to produce an ellipsoid analogous to an optical indicatrix surface. This ellipsoidal surface provides a convenient parameter that describes the preferred crystallographic orientation. The magnitude and directional cosines of the ellipsoidal axes are listed in Table 1 and are shown in Figure 1.

The three velocity measurements V_1, V_2, and V_3, which are referred to as a data set, were taken over nine directions. Each data set was replicated 4 times for each direction, the result

TABLE 2. Q_i Values

Replicate	Propagation Direction 1	2	3	4	5	6	7	8	9
				Quartzite (F = 50.11)					
1	49.581	52.443	53.968	54.851	53.629	55.214	50.649	55.575	51.071
2	50.943	53.084	54.484	55.009	54.027	55.250	52.278	55.643	51.134
3	51.021	53.103	54.248	55.331	54.113	55.668	52.578	55.748	51.989
4	50.872	53.396	54.960	55.132	54.746	55.725	52.900	56.458	51.679
				Marble (F = 64.75)					
1	48.133	38.617	48.049	41.396	37.184	41.716	43.176	44.424	46.309
2	48.089	39.060	45.401	42.308	37.476	41.501	42.953	44.080	42.994
3	49.645	38.136	45.844	42.160	37.999	41.411	42.803	45.482	47.332
4	49.465	38.576	45.989	42.068	37.850	42.058	43.576	45.837	47.171
				Granite (F = 73.20)					
1	55.303	60.130	58.411	59.496	60.608	57.881	57.322	59.896	59.282
2	56.157	60.051	58.994	59.227	60.330	57.057	56.915	60.098	59.828
3	56.115	59.936	58.217	58.947	59.809	57.142	57.936	59.895	59.812
4	55.851	59.623	58.954	58.872	60.308	58.098	57.447	60.271	59.888

being 36 data sets. The order in which the data sets were measured was randomized. The Q_i values from these data sets were determined according to (1) and are listed in Table 2. The mean velocities for each direction (Table 3) were used in computing the Q ellipsoid. The magnitude and directional cosines of the least squares Q ellipsoid axes are listed in Table 4 in the section on quartzite. The plot of these axes is shown in Figure 1. The mean Q_i values with their respective Q_{LS_i} values are listed in Table 5. This table also presents the $\sigma_{\bar{m}}$, $\sigma_{\bar{m}_e}$, and σ_e values. The maximum P wave velocity observed $V_{P\ max}$ is shown in Figure 1.

TABLE 3. Directional Cosines and Mean Velocities

Propagation Direction	Directional Cosines	Mean Velocity, km/sec V_1	V_2	V_3
	Quartzite			
1	(1, 0, 0)	5.110	3.436	3.561
2	(0, 1, 0)	5.206	3.659	3.537
3	(0, 0, 1)	5.332	3.598	3.611
4	(-0.602, 0.0, 0.800)	5.377	3.517	3.715
5	(0.574, 0.0, 0.819)	5.357	3.561	3.571
6	(0.0, -0.652, 0.758)	5.399	3.719	3.533
7	(-0.602, -0.800, 0.0)	5.261	3.548	3.440
8	(0.0, 0.663, 0.749)	5.389	3.668	3.655
9	(0.663, -0.749, 0.0)	5.325	3.553	3.239
	Marble			
1	(1, 0, 0)	5.575	3.059	2.897
2	(0, 1, 0)	4.711	2.835	2.892
3	(0, 0, 1)	5.387	2.852	3.026
4	(0.0, 0.707, 0.707)	5.028	2.792	2.985
5	(0.0, -0.707, 0.707)	4.634	2.799	2.885
6	(-0.707, 0.707, 0.0)	5.009	2.826	2.931
7	(0.707, 0.707, 0.0)	5.114	2.855	2.970
8	(-0.707, 0.0, 0.707)	5.273	3.029	2.823
9	(0.707, 0.0, 0.707)	5.397	3.019	2.773
	Granite			
1	(1, 0, 0)	5.684	3.425	3.438
2	(0, 1, 0)	5.882	3.505	3.612
3	(0, 0, 1)	5.775	3.498	3.614
4	(0.0, 0.623, 0.783)	5.819	3.544	3.555
5	(0.0, -0.643, 0.766)	5.931	3.543	3.540
6	(0.469, 0.0, 0.883)	5.728	3.571	3.461
7	(-0.530, 0.0, 0.848)	5.786	3.556	3.358
8	(0.415, 0.910, 0.0)	5.880	3.537	3.600
9	(-0.446, 0.895, 0.0)	5.860	3.507	3.614

Grenville marble. The results of the optical petrofabric analysis on the marble are shown in Figure 2. Since the marble displayed a strong preferred orientation, the c axes, ⟨0001⟩, were contoured according to the Mellis method [*Turner and Weiss*, 1963]. The observed micaceous layering is in the N-S vertical plane. The c axes were space-averaged (Table 1, section on

TABLE 4. Q Ellipsoid Axes

Magnitude	Directional Cosines	Symbol
	Quartzite	
56.010	(-0.097, -0.082, 0.992)	M_g
50.539	(0.975, -0.184, 0.127)	m_g
53.243	(0.172, 0.979, 0.097)	I_g
	Marble	
48.048	(0.988, 0.088, 0.128)	M_g
36.679	0.062, -0.970, 0.236)	m_g
44.947	(-0.145, 0.225, 0.964)	I_g
	Granite	
60.644	(-0.034, -0.995, 0.090)	M_g
55.792	(0.994, 0.015, 0.112)	m_g
58.306	(-0.113, 0.079, 0.988)	I_g

TABLE 5. Q_i, Q_{LS_i}, and Deviation Values

Propagation Direction	Quartzite*		Marble†		Granite§	
	Q_i	Q_{LS_i}	Q_i	Q_{LS_i}	Q_i	Q_{LS_i}
1	50.602	50.601	48.829	47.887	55.856	55.753
2	53.005	53.254	38.596	37.308	59.935	60.558
3	54.414	55.993	46.311	44.478	58.643	58.528
4	55.081	54.617	41.982	43.071	59.135	58.777
5	54.128	53.654	37.627	38.716	60.263	59.910
6	55.464	54.611	41.671	41.870	57.543	57.919
7	52.097	52.509	43.126	43.325	57.401	57.747
8	56.856	55.006	44.950	45.694	60.040	59.826
9	51.467	51.866	45.928	46.671	59.702	59.501

*σ_M = 1.759; $\sigma_{\bar{m}}$ = 1.601; σ_e = 0.728.
†σ_M = 3.463; $\sigma_{\bar{m}}$ = 3.308; σ_e = 1.026.
§σ_M = 1.417; $\sigma_{\bar{m}}$ = 1.377; σ_e = 0.335.

marble), and the axes of the optical indicatrix type surface are plotted in Figure 2.

Twelve velocity measurements in nine independent directions were taken, and the Q_i values were calculated (Table 2). From the mean velocities (Table 3) the Q ellipsoid was determined. The directional cosines and the magnitudes of the ellipsoidal axes are listed in Table 4 in the section on marble. The plot of these axes is shown in Figure 2. The Q_i and Q_{LS_i} values were derived as $\sigma_{\bar{m}}$, $\sigma_{\bar{m}e}$, and σ_e were and are listed in Table 5. The observed maximum P wave velocity is shown in Figure 2.

Granite boulder. Velocity measurements of the granite were used to compute the Q_i values (Table 2, section on granite). From the mean velocities (Table 3) the Q ellipsoid was determined (Table 4, section on granite). The axes of the Q ellipsoid are plotted in Figure 3. The Q_i and Q_{LS_i} values, along with $\sigma_{\bar{m}}$, $\sigma_{\bar{m}e}$, and σ_e, are listed in Table 5. The observed maximum P wave velocity is plotted in Figure 3.

The orientation of the Q ellipsoid relative to the boulder shape is shown in Figure 3. The axes orientation of the shape ellipsoid was measured to an estimated accuracy of $\pm 10°$.

It should be pointed out that for single crystals of quartz and calcite the representative optic and sonic surfaces are opposite in sign. Therefore in crystal aggregates a maximum optic axis might reasonably correspond to a minimum sonic axis.

CONCLUSIONS

For all samples investigated the calculated Q_i values for each direction display an F value significant at the 0.01 confidence level (Table 2). This indicates that the quartzite, marble, and granite are seismically anisotropic. The sum of the squares of the three seismic wave type velocities over the nine measured directions describes an ellipsoidal surface and satisfies the conditions of equation 8 (Table 5). Thus the seismic anisotropy of the samples observed in Table 2 results from the behavior of the polycrystalline material as an elastic long-wave equivalent to a single crystal.

For the baraboo quartzite the Q ellipsoid axes and the optical indicatrix type surface axes closely coincide. The maximum angular separation between the principal axes of the two surfaces is 11° or less (Table 6). The optical surface is nearly spherical, the major and minor axes differing in magnitude by only 0.4%, compared with a difference of 2.2% in a single

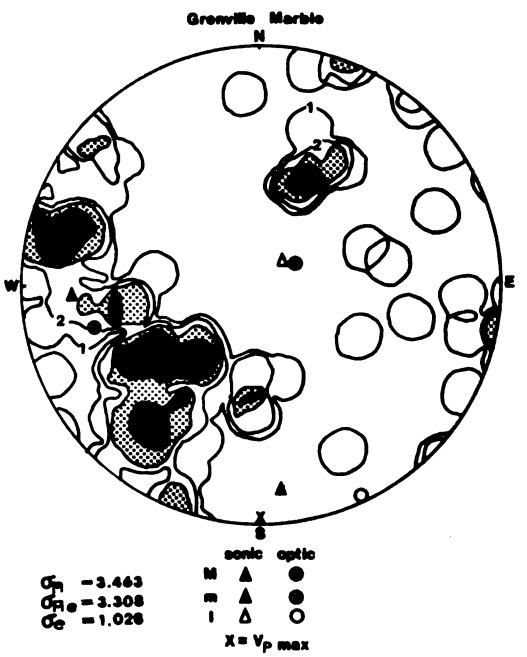

Fig. 2. Equal-area projection of 100 calcite c axes for the Grenville marble contoured by the Mellis method at intervals of 1, 2, 3, and 4% of the axes per 1% area. Stipled areas denote 3% concentrations. Hatchured areas denote greater than 4% concentrations per 1% area. Micaceous layering is in the N-S vertical plane. The observed maximum P wave velocity, optical surface, and Q ellipsoid principal axes are also plotted, M, m, and I being the major, minor, and intermediate axes, respectively, of the ellipsoidal surfaces. Location of the sonic minor axis is the result of interaction between the structural fabric and the crystallographic fabric.

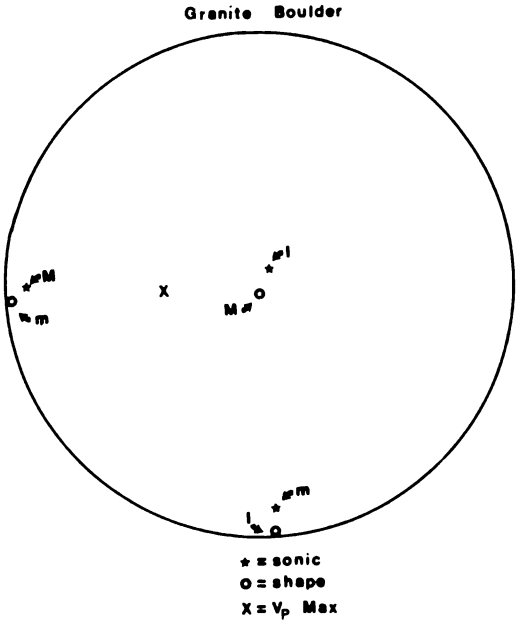

Fig. 3. Projection of the Q ellipsoid and shape ellipsoid principal axes for the plastically deformed granitic boulder. The observed maximum P wave velocity is also shown. Close coincidence between the ellipsoidal axes indicates that the Q ellipsoid technique may be useful in describing regional tectonic forces.

quartz crystal. The near sphericity indicates a weak preferred crystallographic orientation. Statistical analysis of the scatter diagram of Figure 1 yields a correlation coefficient of $r = 0.103$ [*Chayes*, 1949]. Therefore the degree of orientation, as displayed in Figure 1, is not significant at the 0.05 confidence level ($r_{0.05} = 0.200$). It is interesting to note that the calculated correlation coefficient is significant at the 0.10 confidence level ($r_{0.10} = 0.100$). The magnitudes between the major and the minor sonic Q ellipsoid axes differ by 10%, compared with a difference of 18% for a single quartz crystal. We conclude from the study on this sample that the Q ellipsoid method readily detects preferred crystal orientations. The close coincidence between the sonic and the optical surface axes in this nearly optically isotropic sample is strong evidence that the sonic orientation accurately reflects subtle fabric orientation.

The Grenville marble produces a Q ellipsoid whose principal axes describe the effects of structural and crystal fabric. To a first approximation this sample behaves as a layered material, the minimum velocities being normal to the micaceous layering [*Postma*, 1955]. This structural fabric would tend to locate the minor sonic axis at the west pole of Figure 2. The major optical surface axis corresponds to the minor sonic axis (Table 6). Thus the crystal fabric would tend to locate the minor sonic axis coincident with the major optical surface axis. Interaction of these two fabrics would place the minor sonic axis between the west pole and the major optical surface axis. Therefore the observed location of the minor Q ellipsoid axis is as expected (Figure 2). The Q ellipsoid axes differ by 27%, compared with 39% for a single calcite crystal, a rather strongly anisotropic material being indicated.

The principal shape axes and the Q ellipsoid axes of the granite boulder closely coincide (Figure 3). The multiphase granite behaves homogeneously as a pseudosingle crystal oriented in response to plastic deformation. Thus the Q ellipsoid technique may be useful in detecting and describing regional tectonic forces.

For quartzite, marble, and granite the angles between the Q ellipsoid maximum axis and the observed maximum P wave velocity are 36°, 9°, and 45°, respectively (Table 3 and Table 4). For quartzite and marble the P wave velocity measured in the direction nearly coincident with the maximum Q ellipsoid axis was not the observed maximum P wave velocity. Thus the direction of the observed $V_{P\,max}$ has not been a reliable indicator of the Q ellipsoid major principal axis. Indeed it is conceivable that the P wave could indicate sample isotropy, whereas the Q ellipsoid indicates seismic anisotropy [*Bennett*, 1972]. Therefore the use of the P wave velocity surface to determine preferred

TABLE 6. Optical and Sonic Axes Separation

Axes	Separation
Quartzite	
$M_S:I_O$	8°
$m_S:M_O$	11°
$I_S:m_O$	3°
Marble	
$M_S:I_O$	21°
$m_S:M_O$	21°
$I_S:m_O$	4°

crystallographic orientation must be made cautiously.

The results of this study lead us to conclude that (1) the elastic behavior of these rock materials is testable and is shown to be that of a homogeneous pseudosingle crystal, (2) in the samples studied the orientation of the sonic Q ellipsoid is controlled by preferred crystallographic orientations of the materials and by structural effects, (3) weakly preferred orientations are readily observable with the Q ellipsoid method, (4) the sonic Q ellipsoid technique is equally valid for single-phase or multiphase materials, and (5) the P wave velocity surface is not necessarily a reliable indicator of principal anisotropic directions.

Acknowledgment. The authors wish to thank Thomas Vogel for his assistance throughout the course of this study.

REFERENCES

Bennnett, H. F., A simple seismic model for determining principal anisotropic direction, *J. Geophys. Res.*, *77*, 3078–3080, 1972.

Chayes, F., Statistical analysis of three-dimensional petrofabric diagrams, in *Structural Petrology of Deformed Rocks*, edited by H. W. Fairbairn, p. 317, Addison-Wesley, Reading, Mass., 1949.

Nye, J. F., *Physical Properties of Crystals*, p. 164, Oxford at the Clarendon Press, London, 1957.

Postma, G. W., Wave propagation in a stratified medium, *Geophysics*, *20*, 780–806, 1955.

Tilmann, S. E., and H. F. Bennett, Ultrasonic shear wave birefringence as a test of homogeneous elastic anisotropy, *J. Geophys. Res.*, *78*, 7623–7629, 1973.

Turner, F. J., and L. E. Weiss, *Structural Analysis of Metamorphic Tectonites*, p. 62, McGraw-Hill, New York, 1963.

(Received April 13, 1973;
revised August 6, 1973.)